

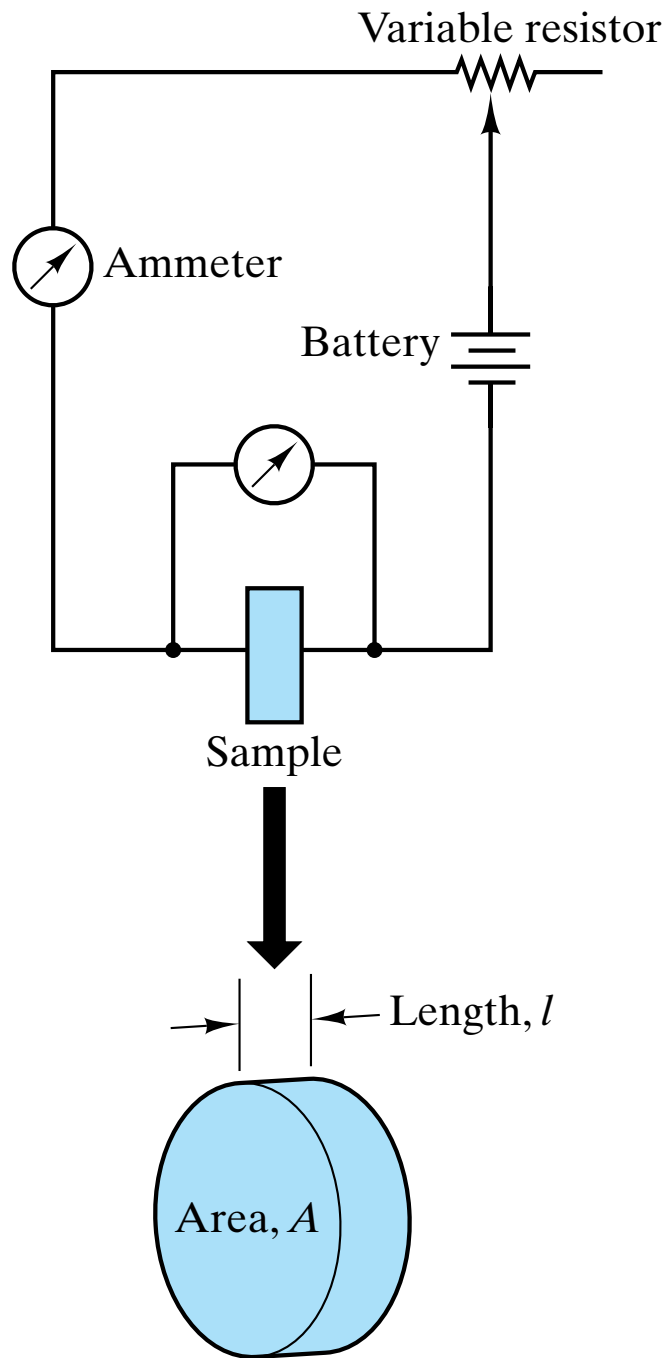
# PART THREE

# CHAPTER 15

## Electrical Behavior

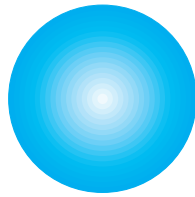
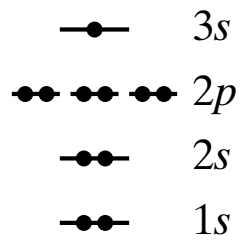


*Electrical behavior is often a critical factor in materials selection. An example is the electrical flex connector seen in the lower left-hand corner of this computer hard disk drive assembly. The metal plate in the disk drive spins at 7200 rpm, generating a temperature between 260 and 315° C. A polyphenylene sulfide (PPS) polymer was chosen for the connector due to its unique combination of good electrical insulation and creep resistance. (Courtesy of Seagate Technology.)*



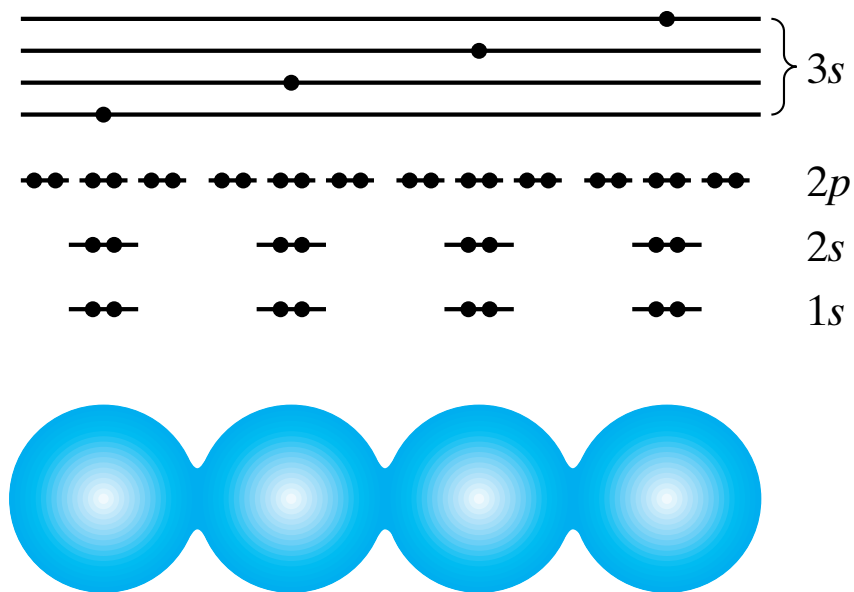
Sample geometry

**Figure 15-1** Schematic of a circuit for measuring electrical conductivity. Sample dimensions relate to Equation 15.2.



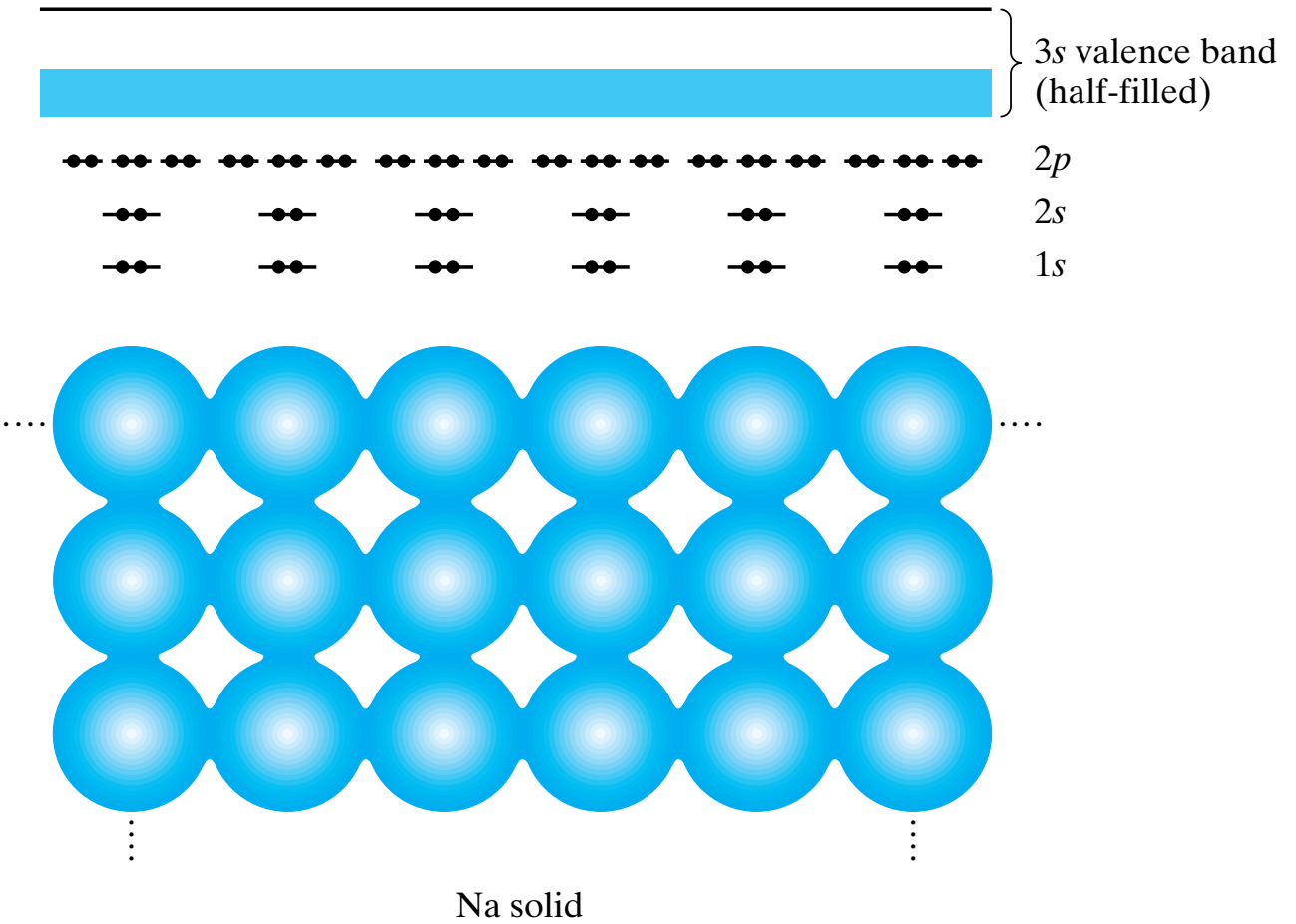
Isolated Na atom

**Figure 15-2** *Energy-level diagram for an isolated sodium atom.*

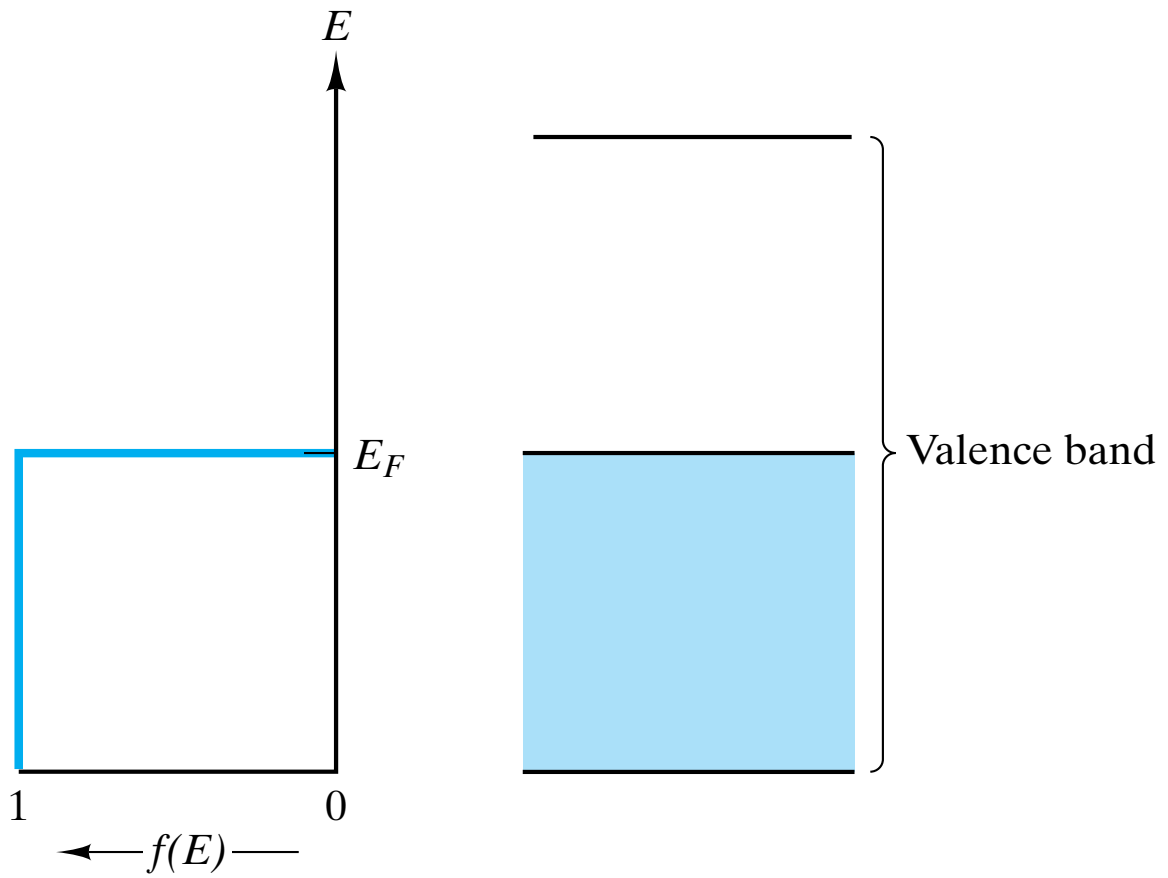


Hypothetical  $\text{Na}_4$  molecule

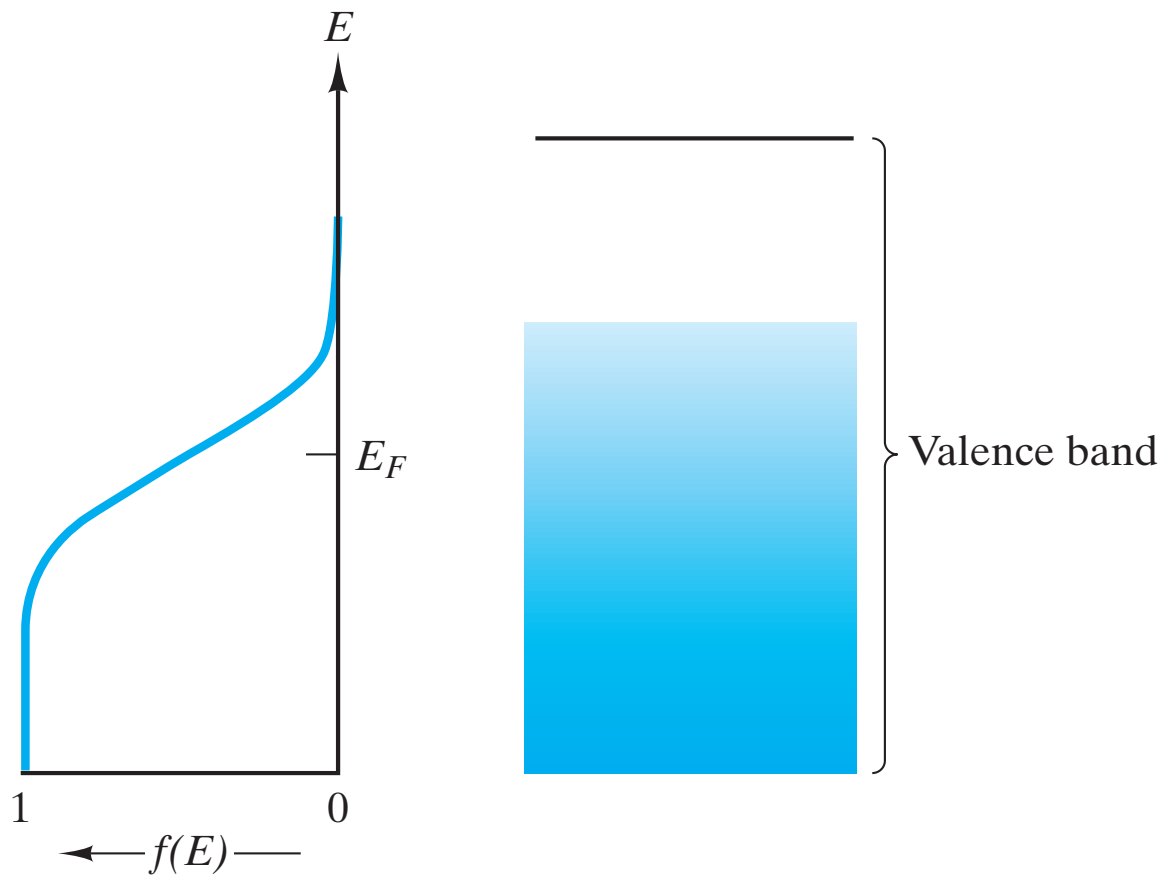
**Figure 15-3** *Energy-level diagram for a hypothetical  $\text{Na}_4$  molecule. The four shared, outer orbital electrons are “split” into four slightly different energy levels, as predicted by the Pauli exclusion principle.*



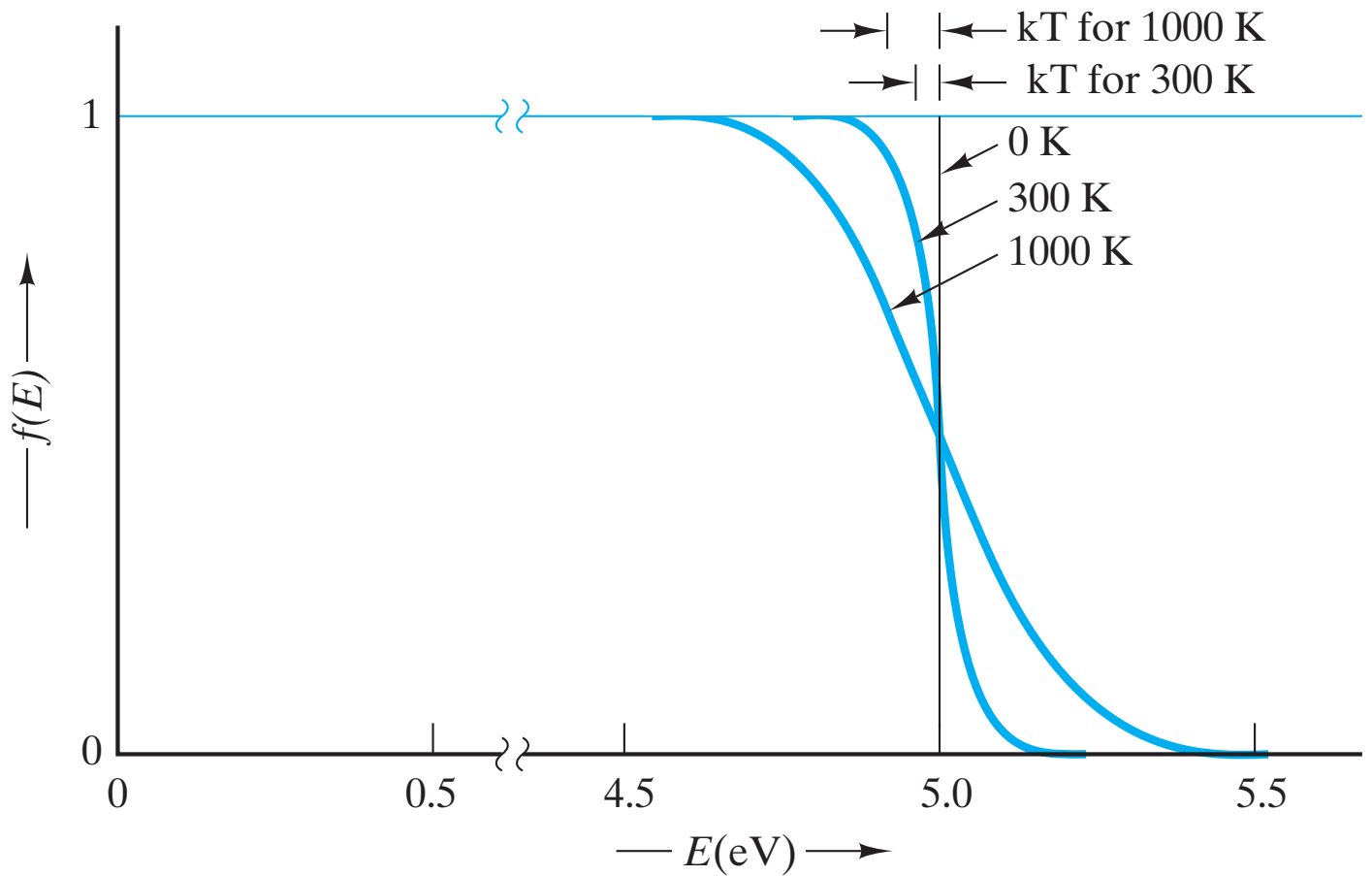
**Figure 15-4** Energy-level diagram for solid sodium. The discrete 3s energy level of Figure 15-2 has given way to a pseudocontinuous energy band (half-filled). Again, the splitting of the 3s energy level is predicted by the Pauli exclusion principle.



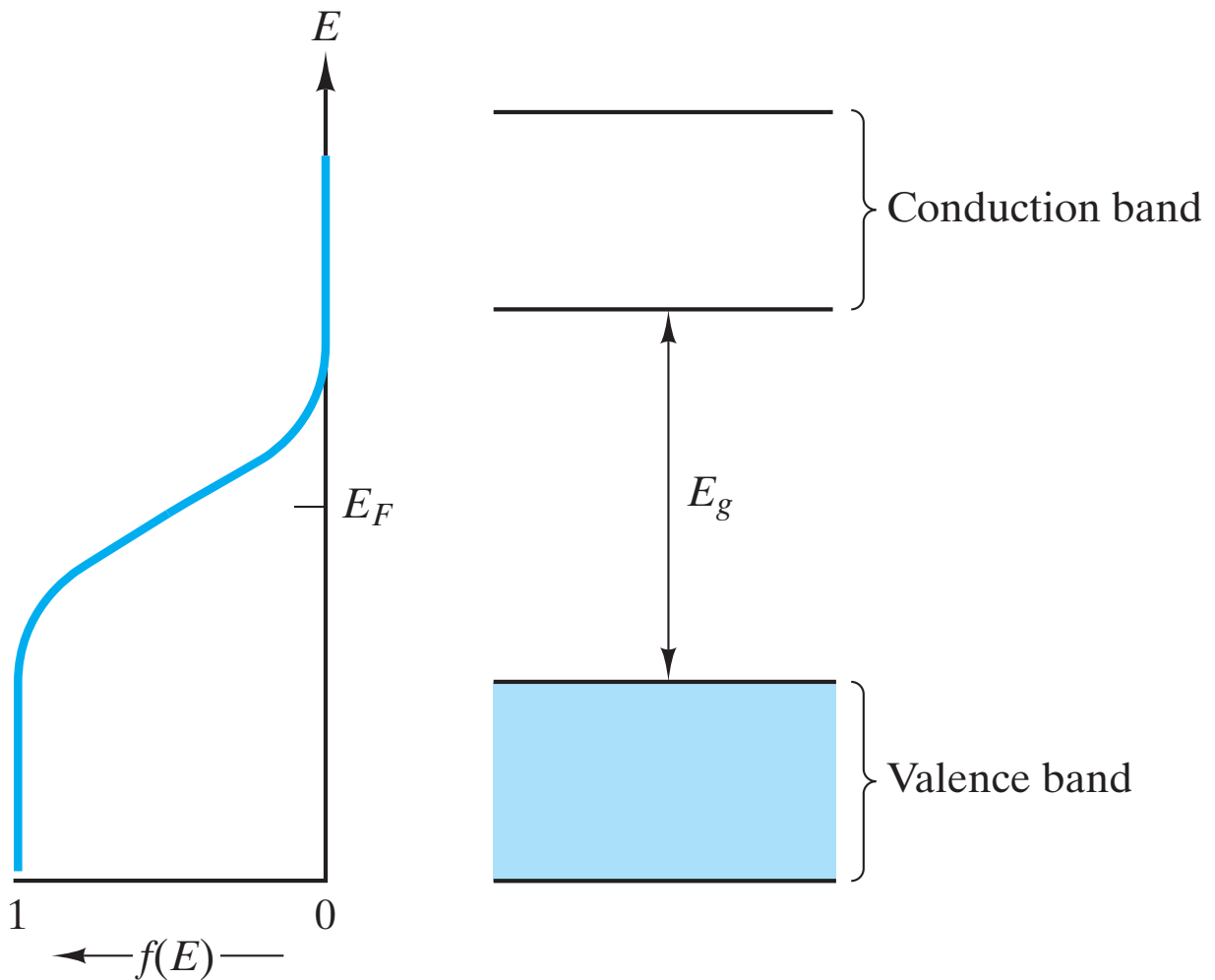
**Figure 15-5** The Fermi function,  $f(E)$ , describes the relative filling of energy levels. At 0 K, all energy levels are completely filled up to the Fermi level,  $E_F$ , and completely empty above  $E_F$ .



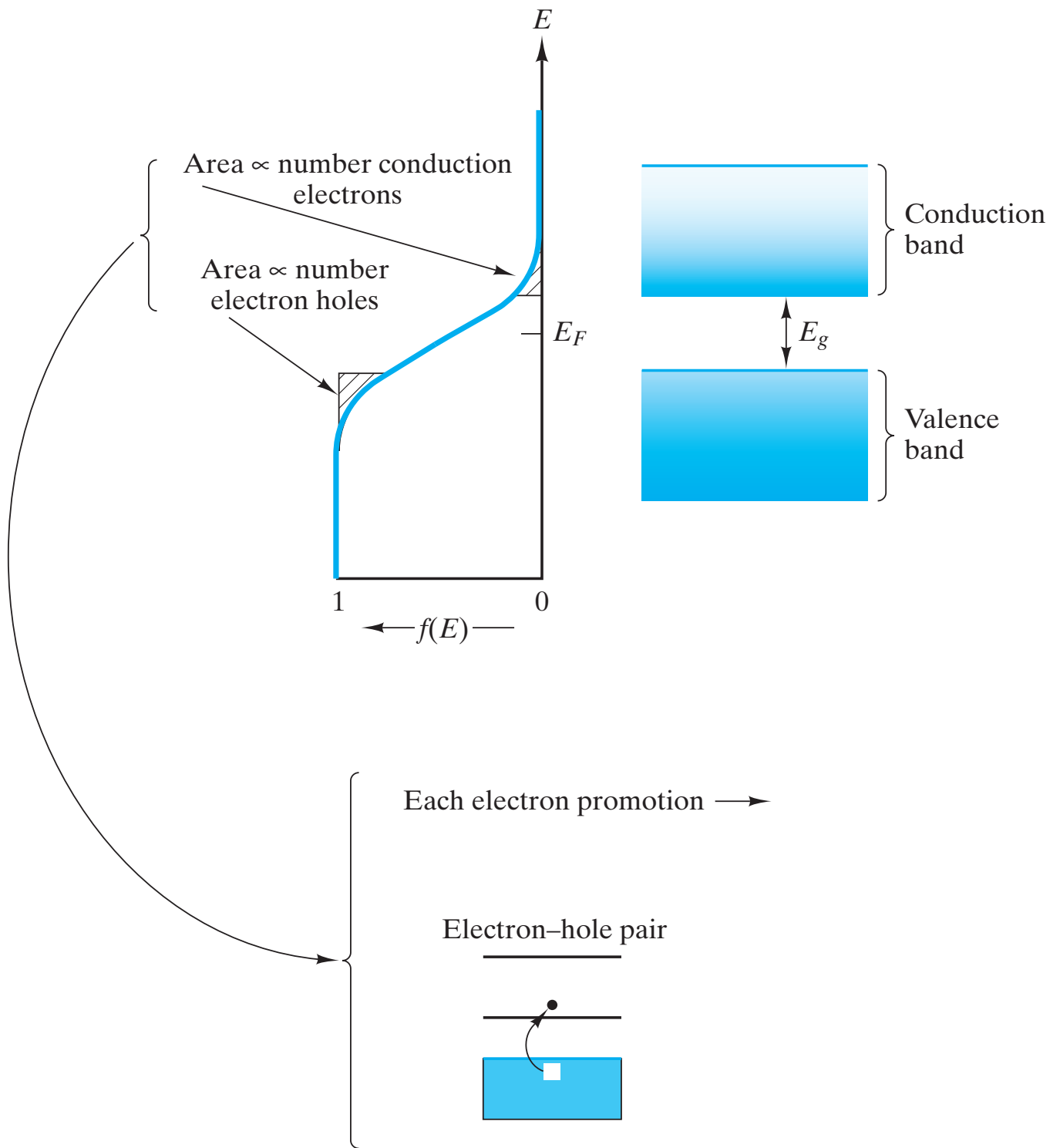
**Figure 15-6** At  $T > 0$  K, the Fermi function,  $f(E)$ , indicates promotion of some electrons above  $E_F$ .



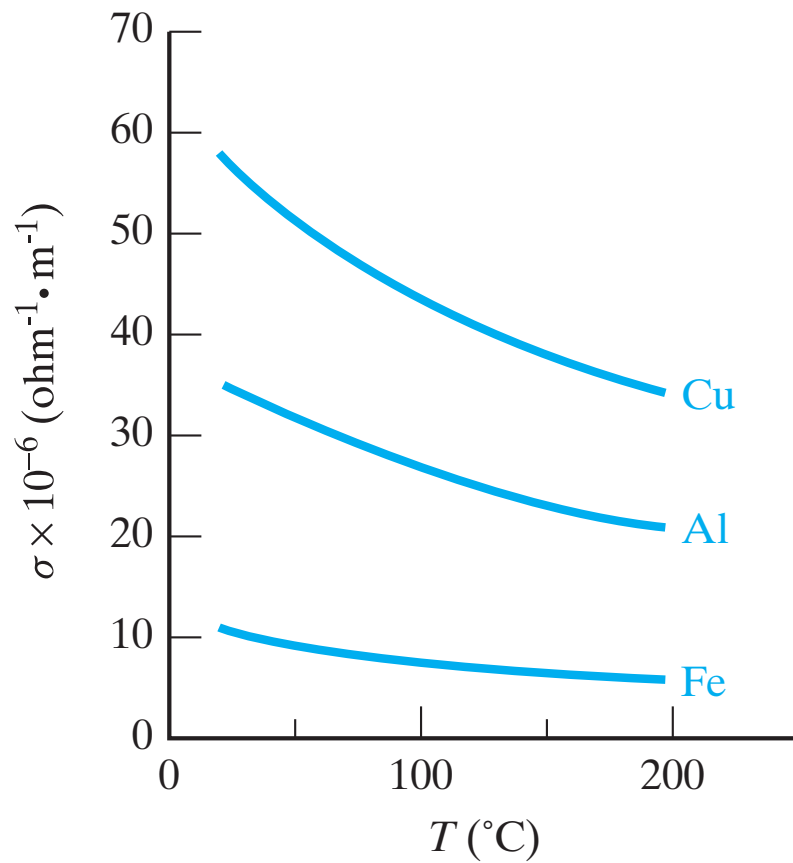
**Figure 15-7** Variation of the Fermi function,  $f(E)$ , with the temperature for a typical metal (with  $E_F = 5$  eV). Note that the energy range over which  $f(E)$  drops from 1 to 0 is equal to a few times  $kT$ .



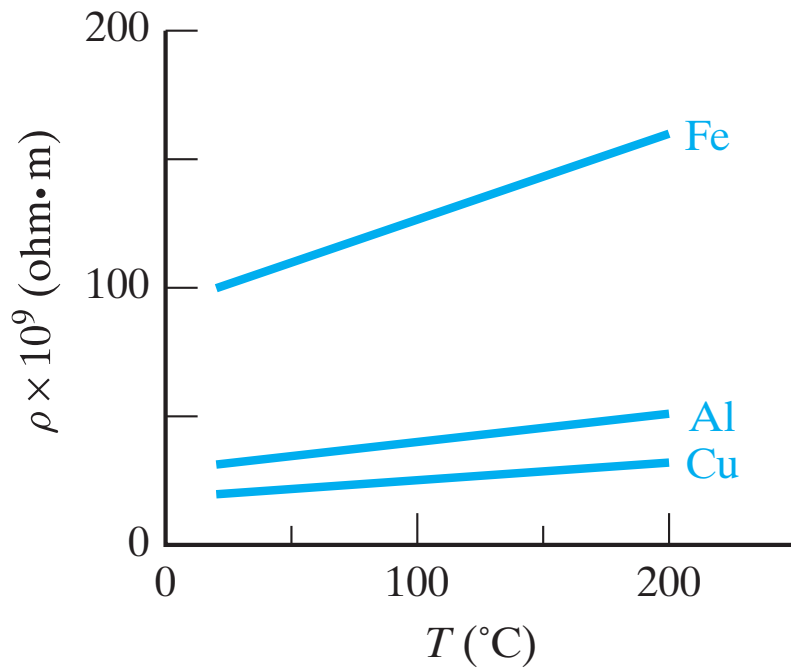
**Figure 15-8** Comparison of the Fermi function,  $f(E)$ , with the energy band structure for an insulator. Virtually no electrons are promoted to the conduction band [ $f(E) = 0$  there] because of the magnitude of the band gap ( $> 2$  eV).



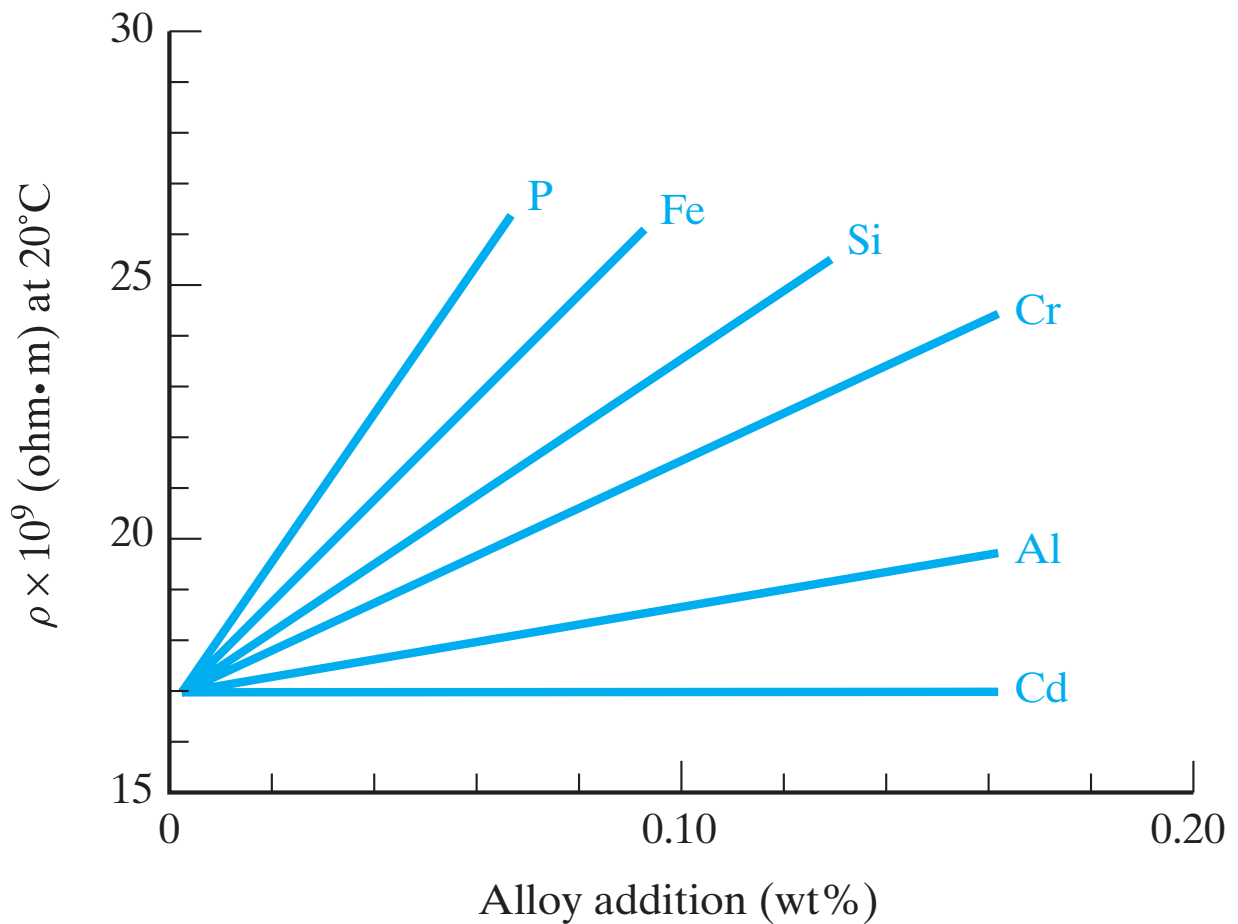
**Figure 15-9** Comparison of the Fermi function,  $f(E)$ , with the energy band structure for a semiconductor. A significant number of electrons is promoted to the conduction band because of a relatively small band gap ( $< 2$  eV). Each electron promotion creates a pair of charge carriers (i.e., an electron-hole pair).



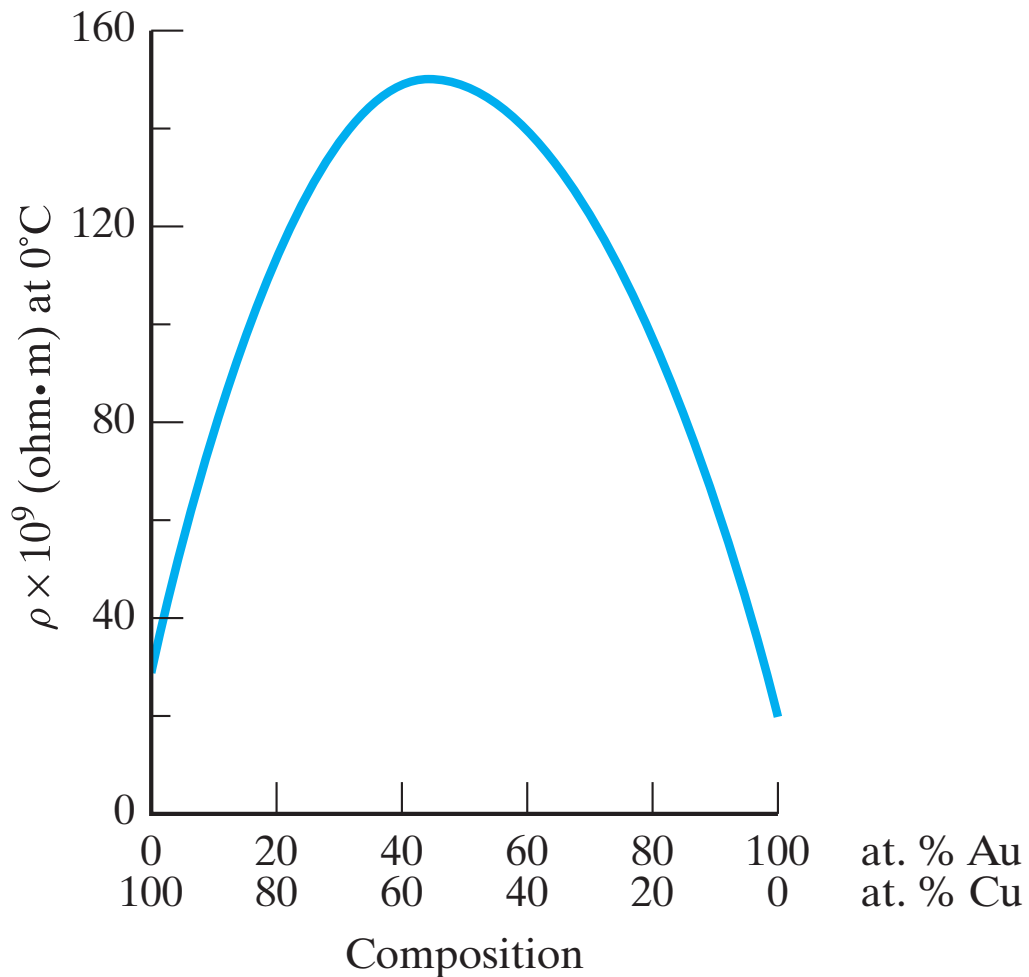
**Figure 15-10** Variation in electrical conductivity with temperature for some metals. (From J. K. Stanley, *Electrical and Magnetic Properties of Metals*, American Society for Metals, Metals Park, Ohio, 1963.)



**Figure 15-11** Variation in electrical resistivity with temperature for the same metals shown in Figure 15-10. The linearity of these data defines the temperature coefficient of resistivity,  $\alpha$ .

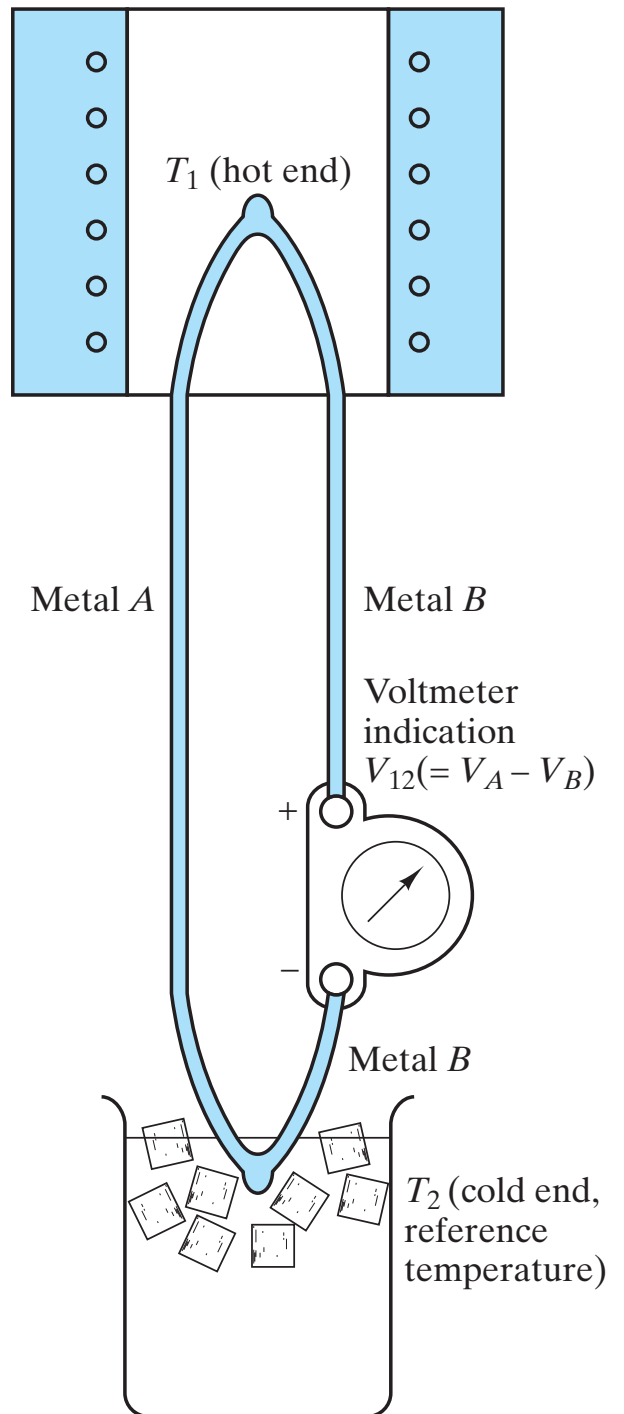


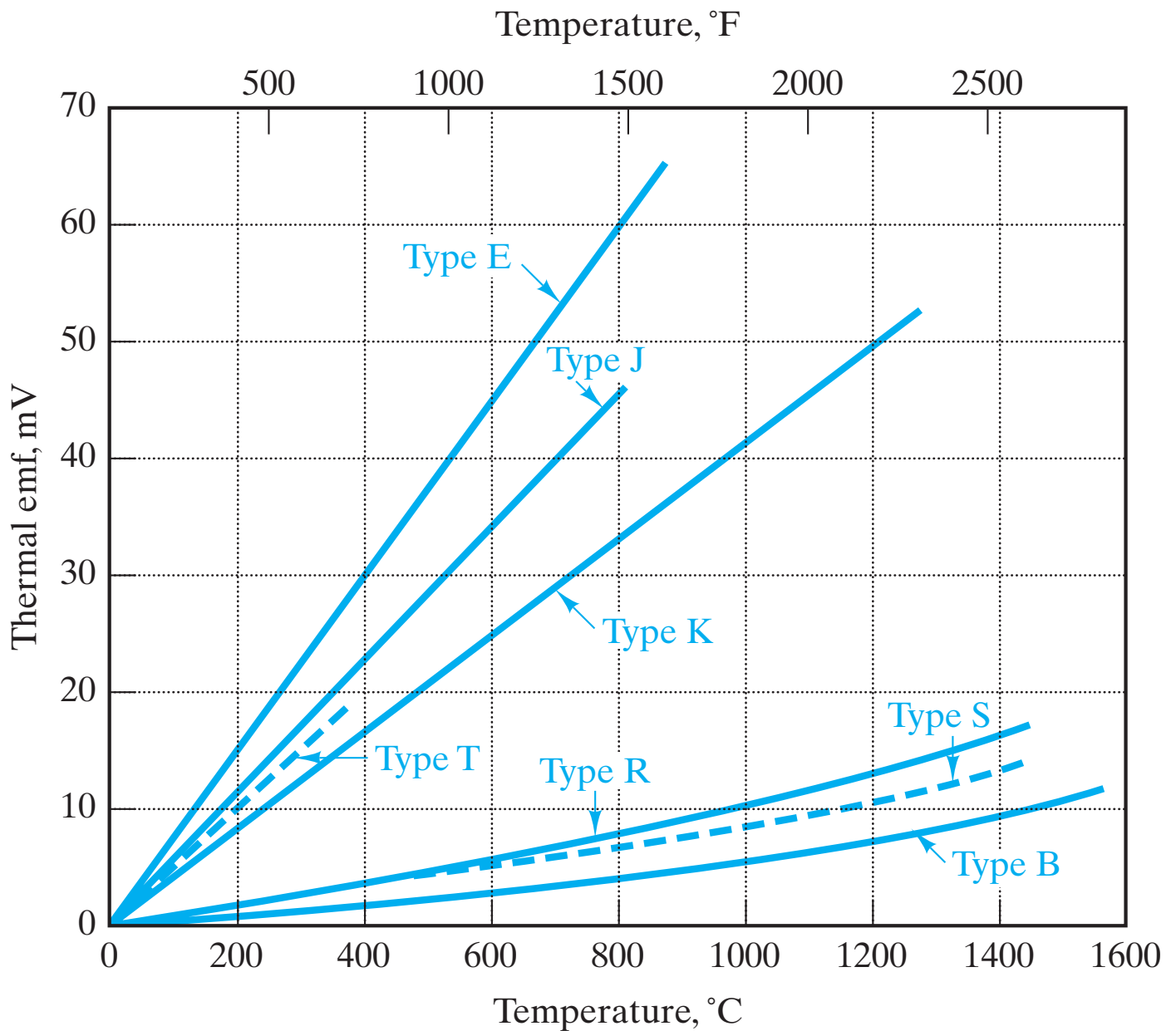
**Figure 15-12** Variation in electrical resistivity with composition for various copper alloys with small levels of elemental additions. Note that all data are at a fixed temperature (20°C). (From J. K. Stanley, *Electrical and Magnetic Properties of Metals*, American Society for Metals, Metals Park, Ohio, 1963.)



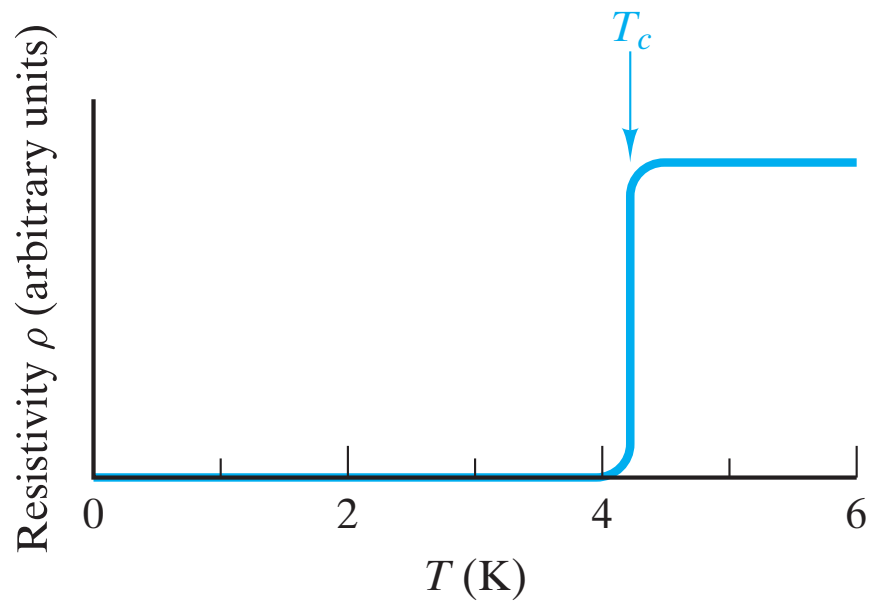
**Figure 15-13** Variation in electrical resistivity with large composition variations in the gold-copper alloy system. Resistivity increases with alloy additions for both pure metals. As a result, the maximum resistivity in the alloy system occurs at an intermediate composition ( $\sim 45$  at % gold, 55 at % copper). As with Figure 15-12, note that all data are at a fixed temperature ( $0^\circ\text{C}$ ). (From J. K. Stanley, *Electrical and Magnetic Properties of Metals*, American Society for Metals, Metals Park, Ohio, 1963.)

**Figure 15-14** Schematic illustration of a thermocouple. The measured voltage,  $V_{12}$ , is a function of the temperature difference,  $T_1 - T_2$ . The overall phenomenon is termed the “Seebeck effect.”

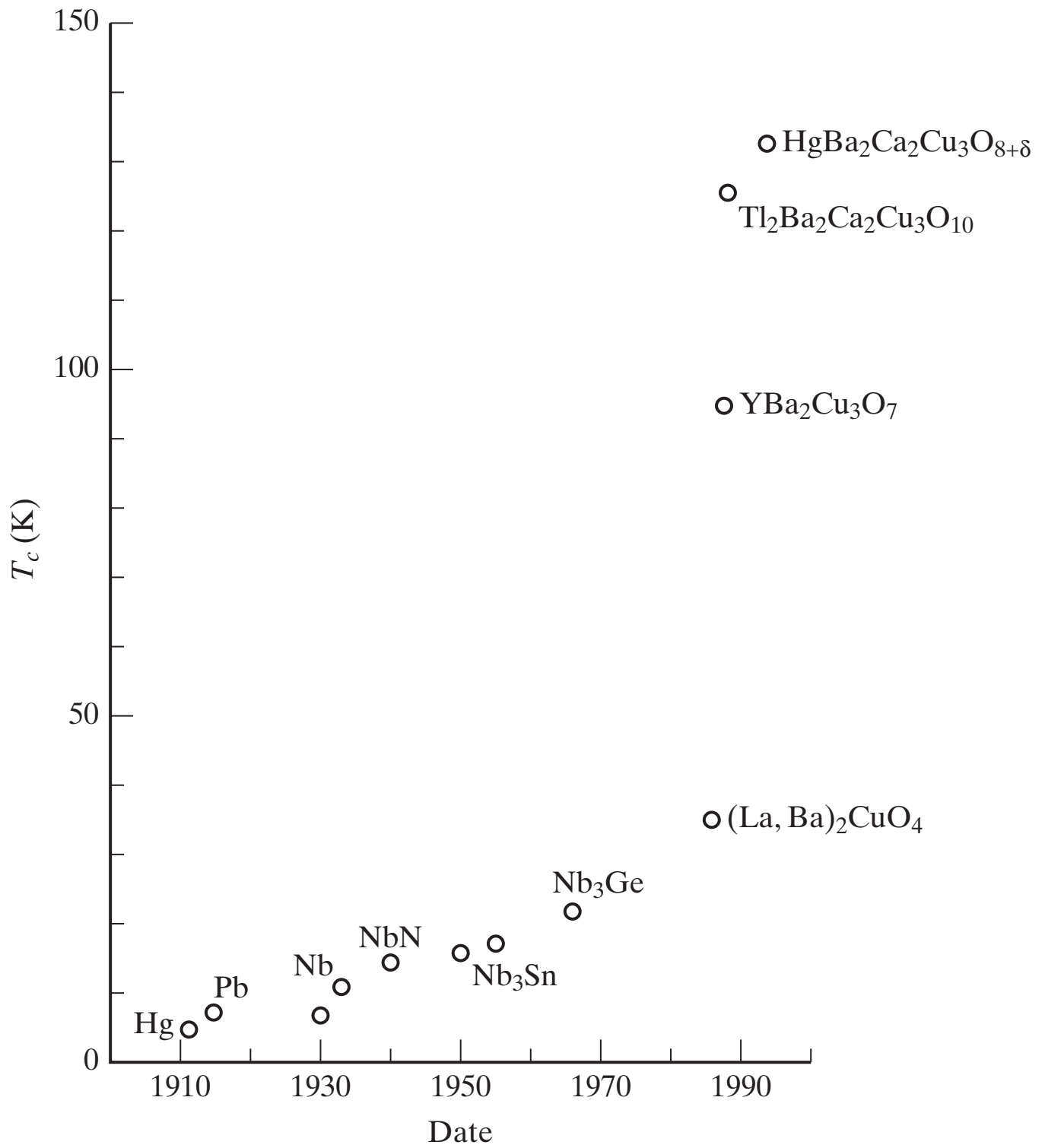




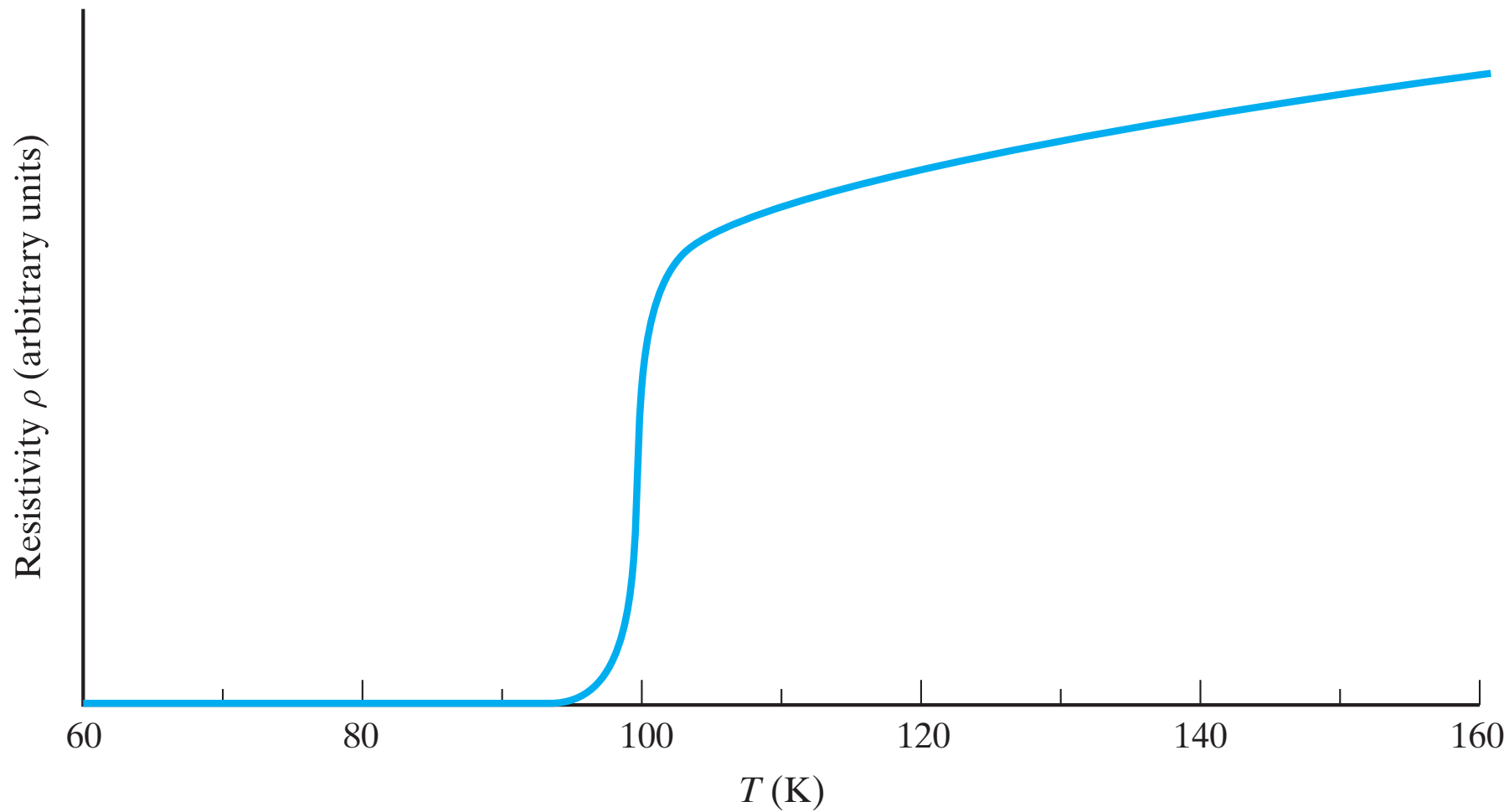
**Figure 15-15** Plot of thermocouple electromotive force ( $= V_{12}$  in Figure 15-14) as a function of temperature for some common thermocouple systems listed in Table 15.3. (From Metals Handbook, 9th ed., Vol. 3, American Society for Metals, Metals Park, Ohio, 1980.)



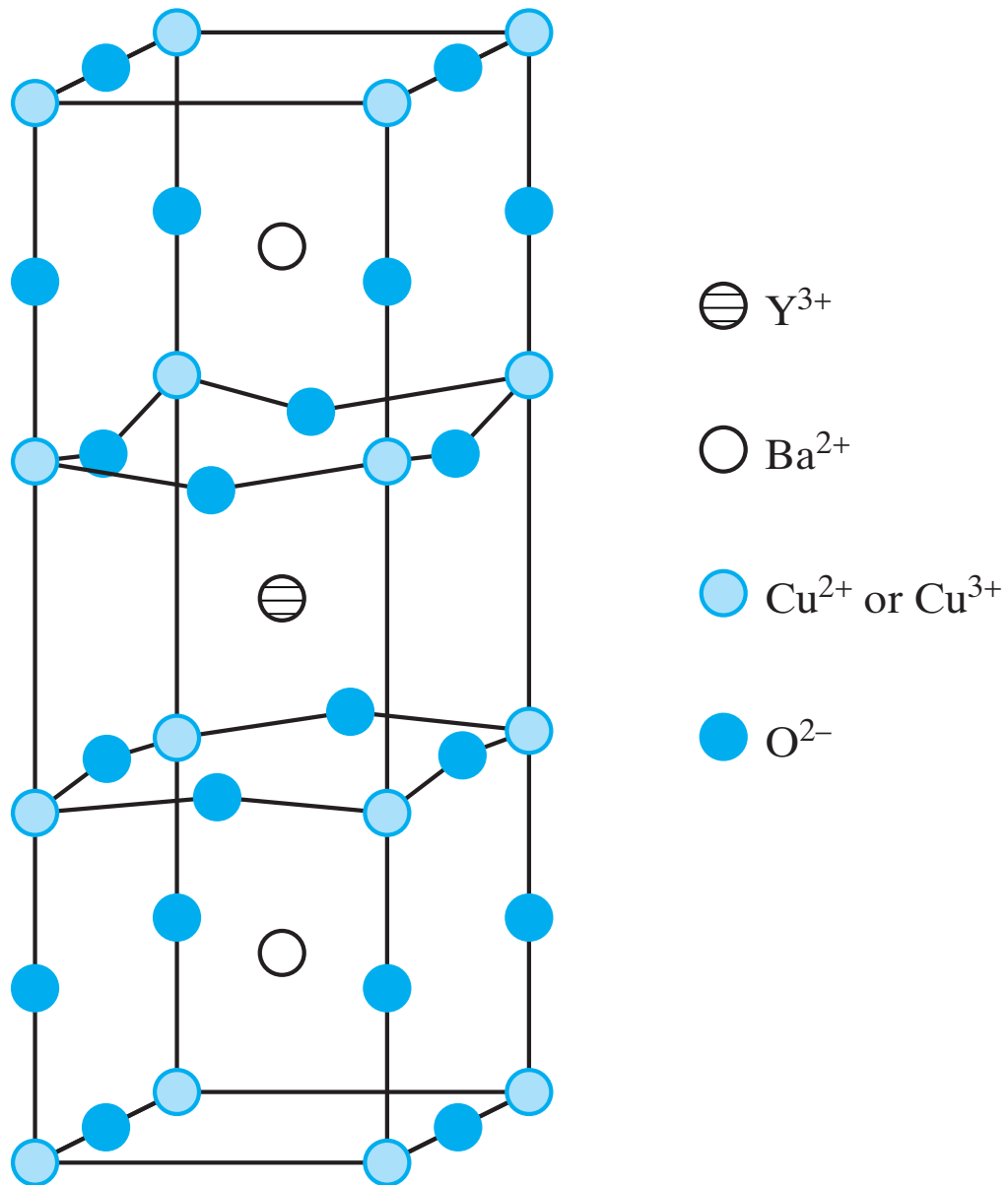
**Figure 15-16** Resistivity of mercury drops suddenly to zero at a critical temperature,  $T_c (= 4.12 \text{ K})$ . Below  $T_c$  mercury is a superconductor.



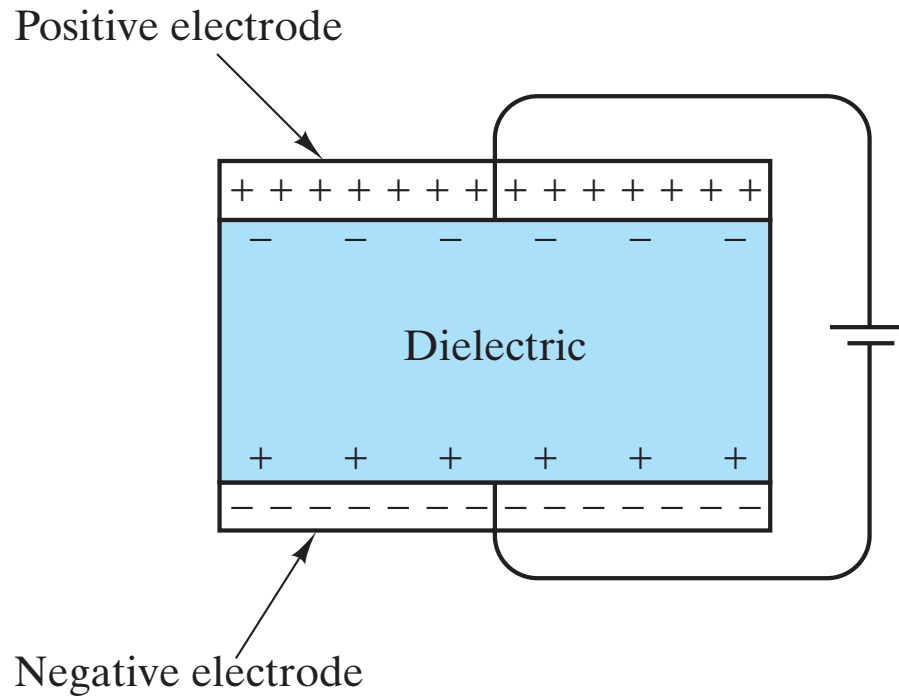
**Figure 15-17** *The highest value of  $T_c$  increased steadily with time until the development of ceramic oxide superconductors in 1986.*



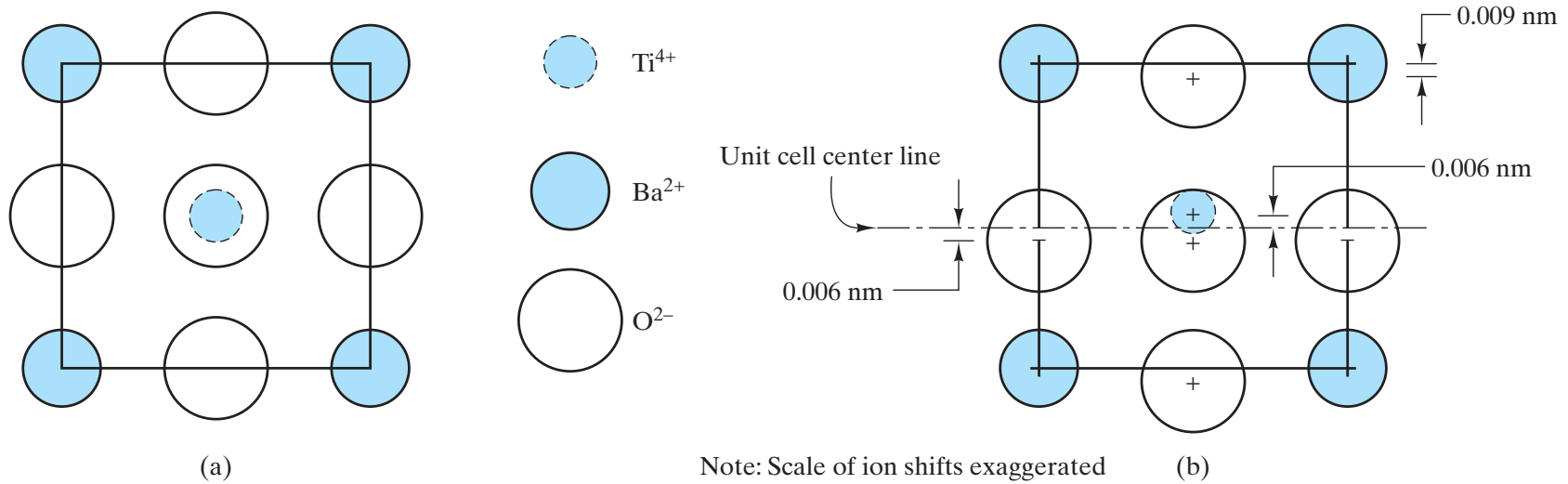
**Figure 15-18** *The resistivity of  $\text{YBa}_2\text{Cu}_3\text{O}_7$  as a function of temperature, indicating a  $T_c \approx 95$  K.*



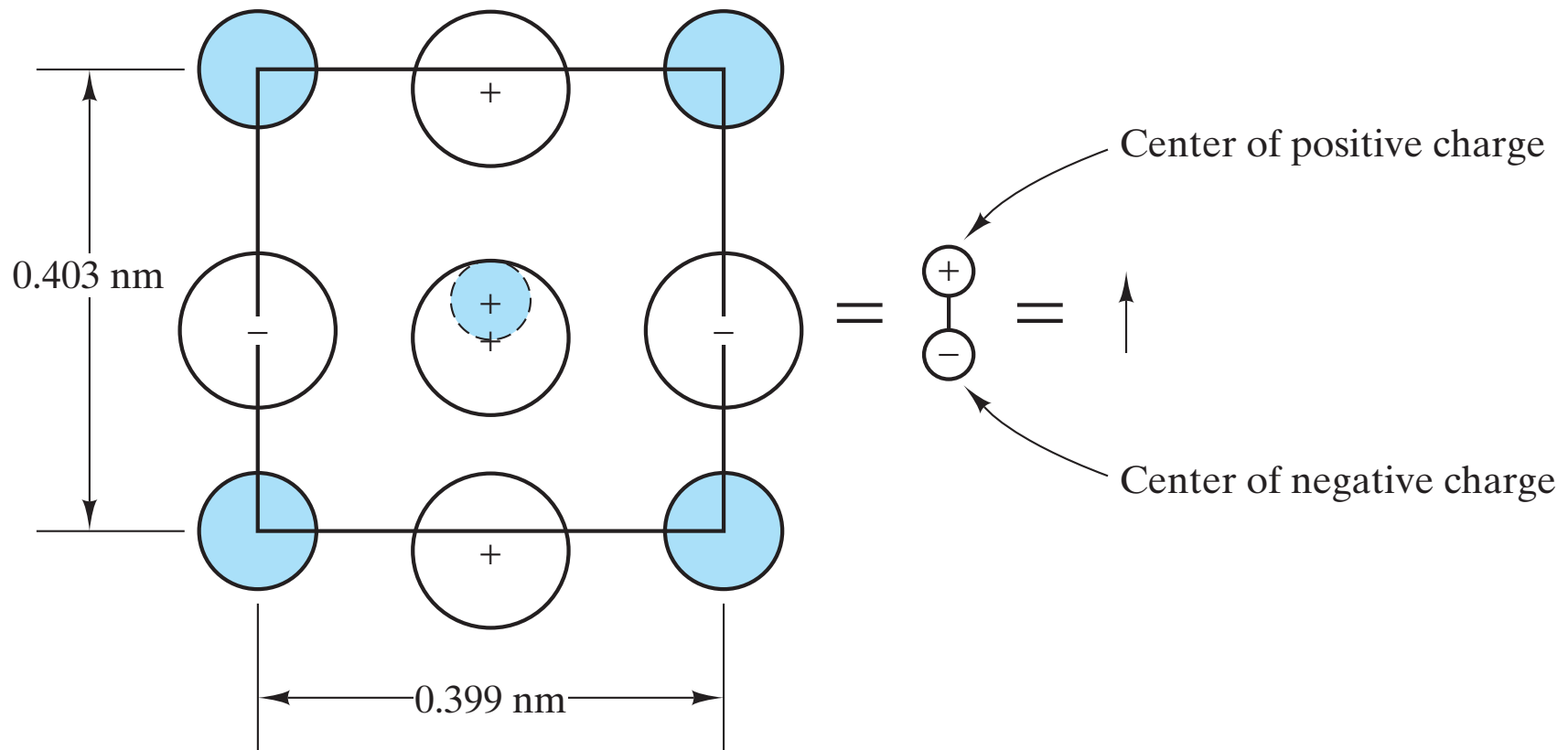
**Figure 15-19** Unit cell of  $\text{YBa}_2\text{Cu}_3\text{O}_7$ . It is roughly equivalent to three distorted perovskite unit cells of the type shown in Figure 3-14.



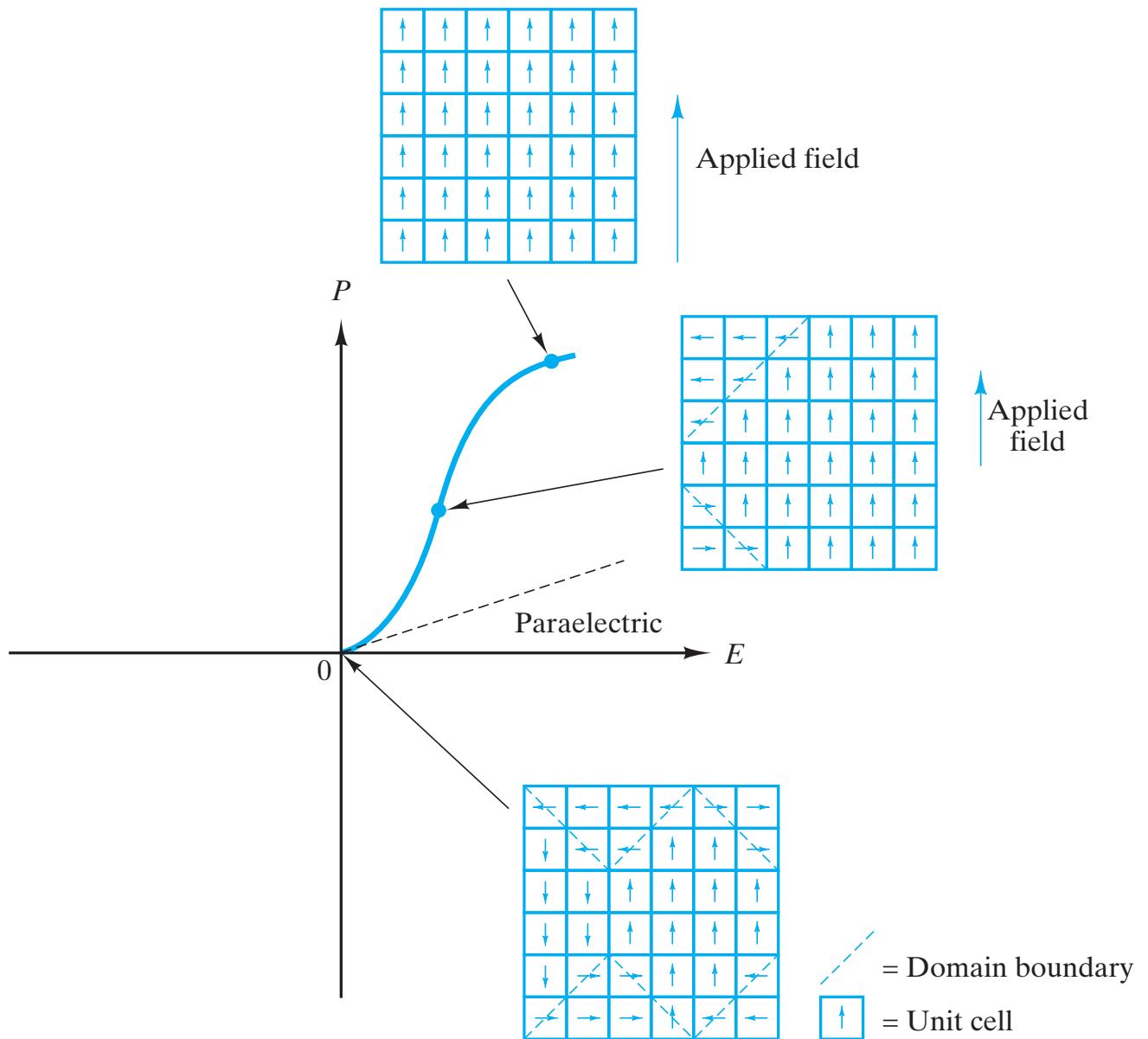
**Figure 15-20** *A parallel-plate capacitor involves an insulator, or dielectric, between two metal electrodes. The charge density buildup at the capacitor surface is related to the dielectric constant of the material, as indicated by Equation 15.13.*



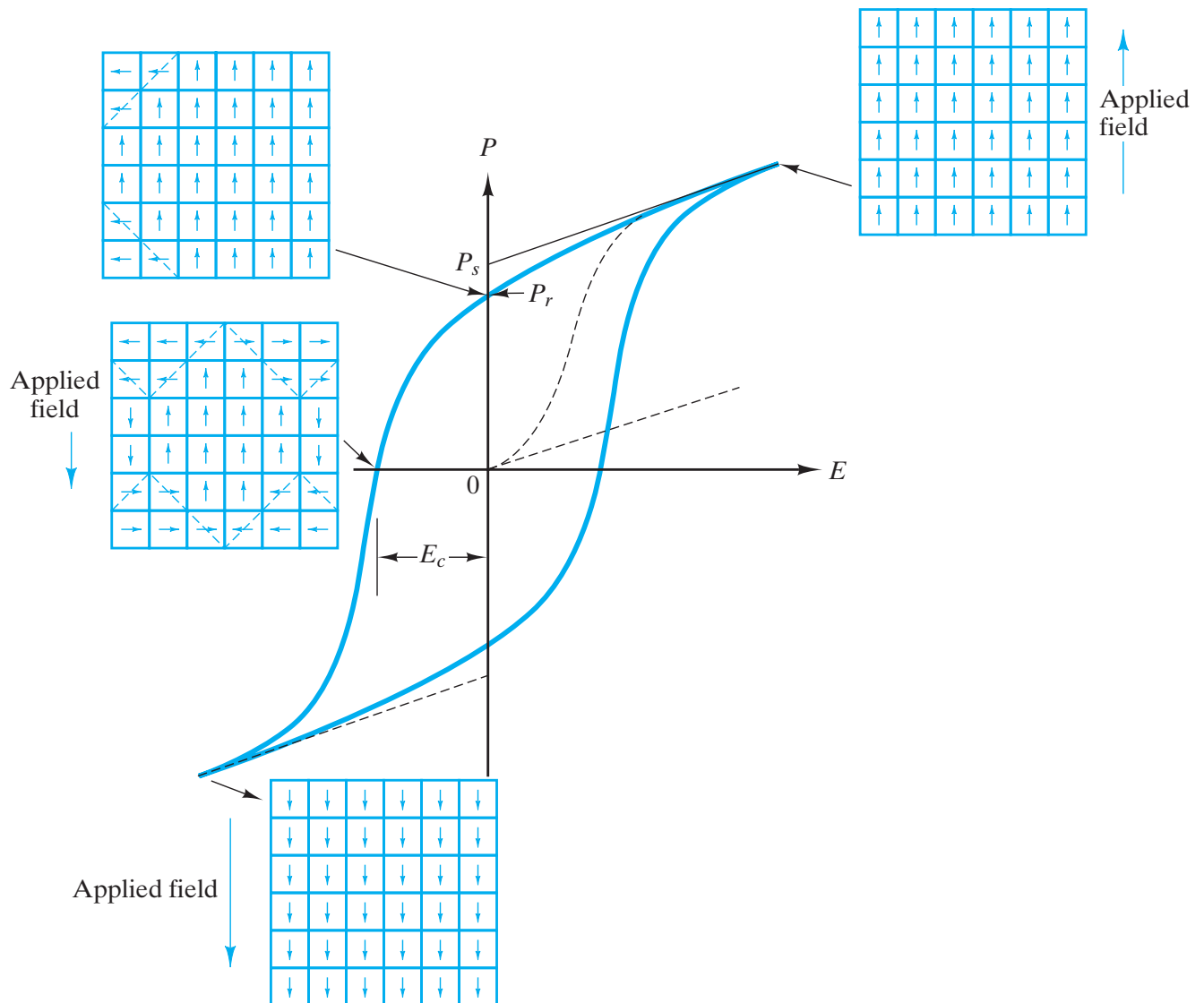
**Figure 15-21** (a) Front view of the cubic BaTiO<sub>3</sub> structure. This can be compared with Figure 3-14. (b) Below 120°C, a tetragonal modification of the structure occurs. The net result is an upward shift of cations and a downward shift of anions.



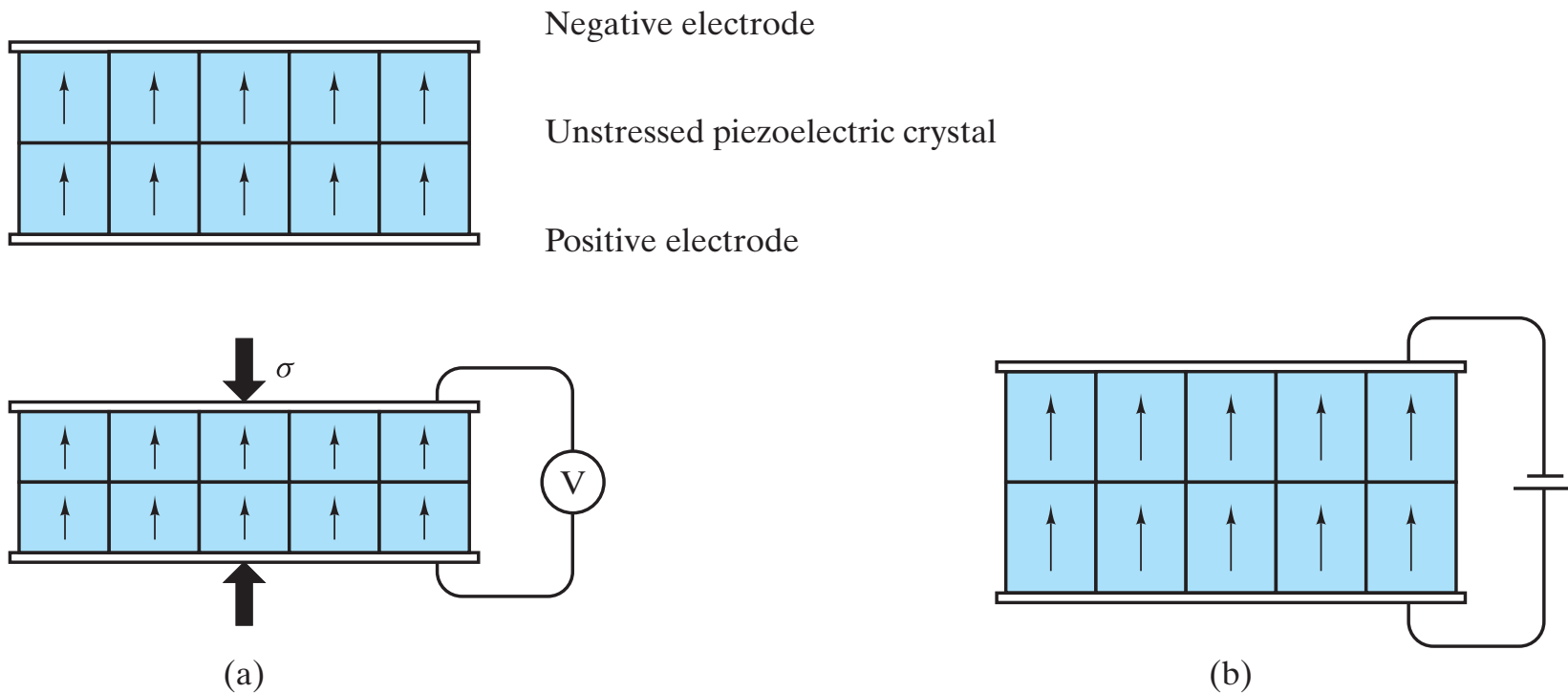
**Figure 15-22** *The tetragonal unit cell shown in Figure 15-21b is equivalent to an electrical dipole (with magnitude equal to charge times distance of separation).*



**Figure 15-23** On a plot of polarization ( $P$ ) versus applied electrical field strength ( $E$ ), a paraelectric material exhibits only a modest level of polarization with applied fields. In contrast, a ferroelectric material exhibits spontaneous polarization in which domains of similarly oriented unit cells grow under increasing fields of similar orientation.

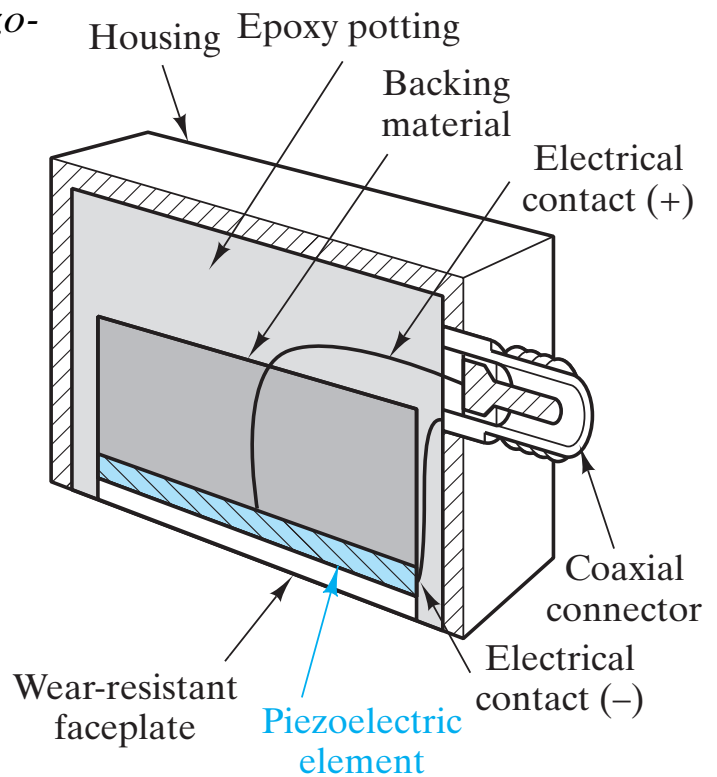


**Figure 15-24** A ferroelectric hysteresis loop is the result of an alternating electric field. A dashed line indicates the initial spontaneous polarization illustrated in Figure 15-23. Saturation polarization ( $P_s$ ) is the result of maximum domain growth (extrapolated back to zero field). Upon actual field removal, some remanent polarization ( $P_r$ ) remains. A coercive field ( $E_c$ ) is required to reach zero polarization (equal volumes of opposing domains).

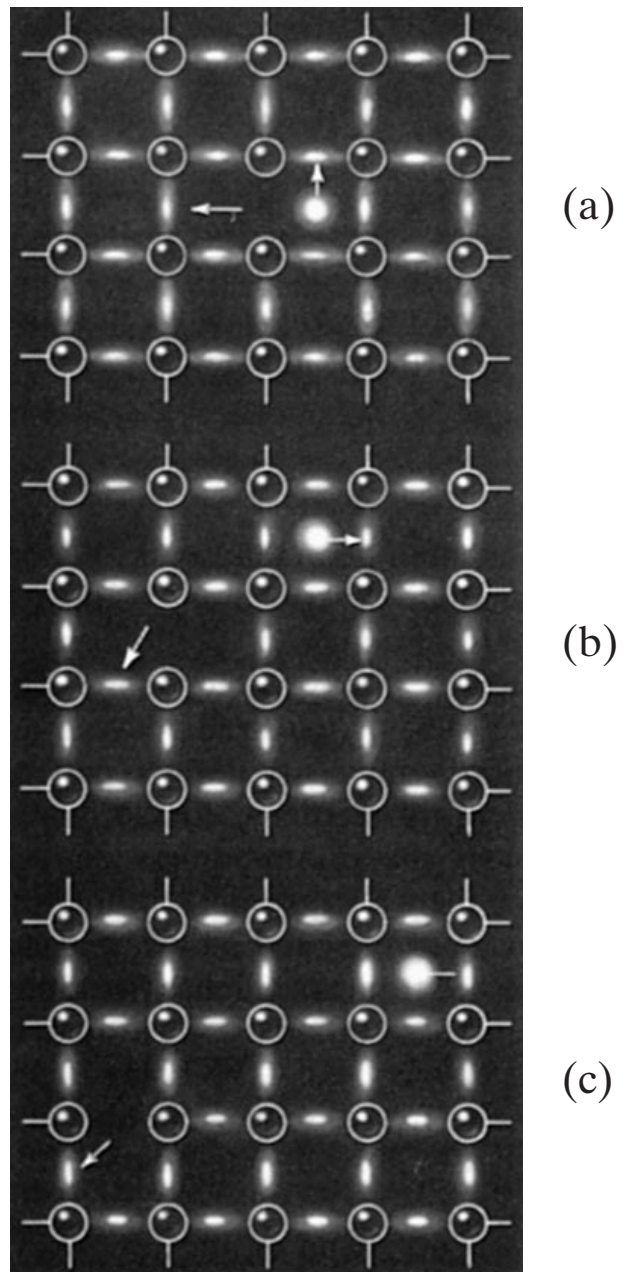


**Figure 15-25** Using schematic illustrations of piezoelectric transducers, we see that (a) the dimensions of the unit cells in a piezoelectric crystal are changed by an applied stress, thereby changing their electrical dipoles. The result is a measurable voltage change. This is the piezoelectric effect. (b) Conversely, an applied voltage changes the dipoles and, thereby, produces a measurable dimensional change. This is the reverse piezoelectric effect.

**Figure 15-26** A common application of piezoelectric materials is in ultrasonic transducers. In this cutaway view, the piezoelectric crystal (or “element”) is encased in a convenient housing. The constraint of the backing material causes the reverse piezoelectric effect (Figure 15–25b) to generate a pressure when the faceplate is pressed against a solid material to be inspected. When the transducer is operated in this way (as an ultrasonic transmitter), an ac electrical signal (usually in the megahertz range) produces an ultrasonic (elastic wave) signal of the same frequency. When the transducer is operated as an ultrasonic receiver, the piezoelectric effect (Figure 15–25a) is employed. In that case, the high-frequency elastic wave striking the faceplate generates a measurable voltage oscillation of the same frequency. (From *Metals Handbook*, 8th ed., Vol. 11, American Society for Metals, Metals Park, Ohio, 1976.)



**Figure 15-27** *Creation and motion of a conduction electron and an electron hole in a semiconductor. (a) An electron breaks away from the covalent bond, leaving a vacant bonding state, or a hole. The electron is now free to move in an electric field. In terms of the band model, the electron has gone from the valence band to the conduction band, leaving a hole in the valence band. The electron is shown moving upward, and the hole to the left. (b) The conduction electron will now move to the right, the hole down to the left. (c) The motions of (b) have been completed; the hole and electron continue to move outward. (From R. M. Rose, L. A. Shepard, and J. Wulff, The Structures and Properties of Materials, Vol. 4: Electronic Properties, John Wiley & Sons, Inc., New York, 1966.)*



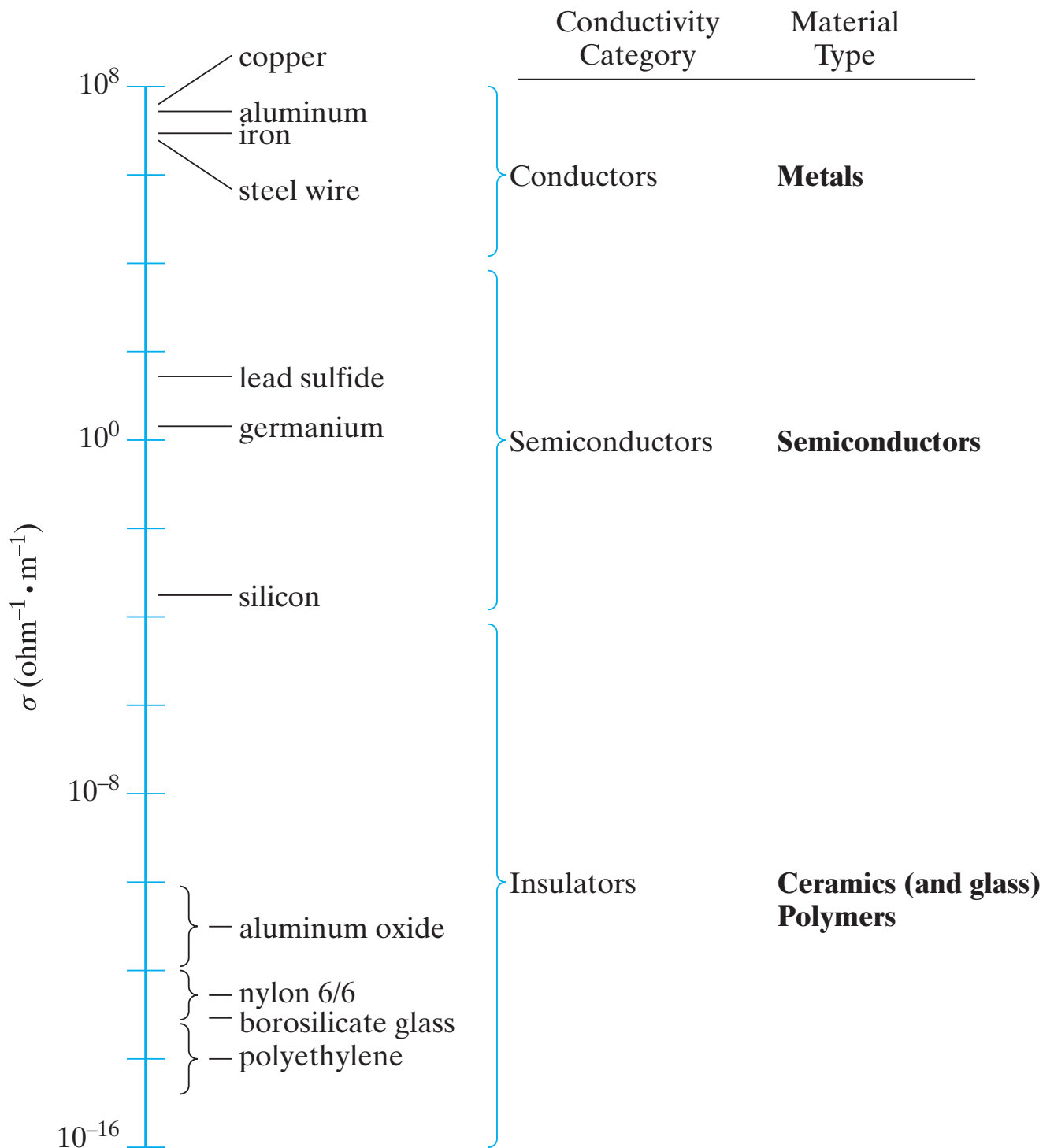


**Figure 15-28** Plot of the electrical conductivity data from Table 15.1. The conductivity ranges correspond to the four fundamental types of engineering materials.